Memoirs of the Faculty of Engineering, Nagoya University
Vol. 27, No. 2 (1975) — Research Report —

FLEXIBLE MOUNTING AND OPTIMUM DAMPING FOR SUPPRESSING ROTOR RESONANCE NEAR CRITICAL SPEEDS

by

HIROSHI ŌTA,* NOBUTAKA MIZUNO** and YASUHIDE KANBE**

(Received November 28, 1975)

Abstract

Analytical results of rotor synchronous response show similar results with the well known ones of dynamic vibration absorber. Designing the flexible support with an appropriate combination of equivalently concentrated mass of pedestal, bearing support stiffness, and optimum damping, the peak amplitude of a rotor-shaft system is found to be kept nearly to the value of rotor eccentricity.

1. Introduction

With the higher revolution of rotary machines and greater performance demanded of machinery, the vibration-proof problem of a rotating shaft becomes of vital importance in this age of high speed machinery.

There inevitably exists a small eccentricity of rotor, or an angle slightly deviated from the ideal mounting. When a gas turbine, a super charger, or a jet engine supported by ball bearings or roller bearings happens to run near its critical speed, the whirling amplitude of the shaft becomes so large that the shaft may break through lack of damping. It is a life or death matter to rotary machinery and to humans whose lives often depend on the proper function of rotary machinery.

Some experiments [1] [2] have been reported which involve the introduction of solid friction or viscous type damping into the housing of rolling element bearings, the outer races of which are supported by rubber or laminated leaf spring which yield both elastic forces and damping forces. It is regrettable that these experimental results were not yet compared with analytical results. Although a number of damped and undamped flexibly mounted bearings have been employed on gas

* Assistant Professor, Department of Mechanical Engineering,
** Mechanical Engineer, Toyota Motor Company Ltd.,

turbines, little analysis [3] [4] [5] has been presented in the literature as to the desirable range of bearing stiffness and damping coefficient that bearing supports should possess in order to minimize the rotor amplitudes over a given wide speed range. For the simplest rotor system fully possessing the dynamical properties of rotor, i. e., gyroscopic effects, we consider in this paper a system having six degrees of freedom in which a rigid rotor is fixed on a massless elastic shaft, and its displacement couples with the inclination angle. One ball bearing of both shaft ends is mounted in an isotropically leastic support, and is also connected orthogonally to the two viscous type dashpots of equal damping. By considering lateral vibrations of bearing support mass, this rotor-shaft system must be treated as a system having six degrees of freedom.

Analytical results of the rotor synchronous unbalance response show similar results with the well known ones of dynamic vibration absorber, i. e., a rectilinear vibratory system having two degrees of freedom [6]. Designing the flexible support with appropriate stiffness and optimum damping, it is found that the peak amplitude of rotor resonance passing through fixed points can be kept nearly to the value of rotor eccentricity. Experimental results of the rotor unbalance resonance coincide well with the analytical results.

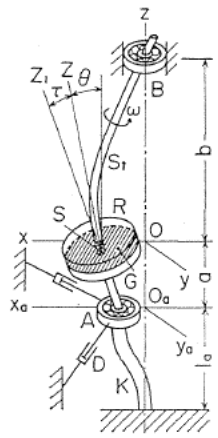

Fig. 1. Schematic view of experimental apparatus.

2. Equations of Motion

This paper deals with the rotating shaft system consisting of a massless elastic shaft St and a rigid rotor R having a mass m. Let O be the position of the geometrical center S of the rotor when no whirl exists, and consider the right-hand rectangular coordinate system O-xyz fixed in space as shown in Fig. 1. Let S (x, y, 0) be the shaft center where the rotor is mounted. The center of lower ball bearing A coincides wiht the origin O_a when the shaft does not whirl. Let a be the distance of the rotor from the lower shaft end A, and b is the distance from the upper shaft end B which is supported in a rigid pedestal; $l=a+b$ shaft length, l_a is the length of flexible support K with isotropical stiffness k_a of lateral deflection at the point A and with an equivalently concentrated mass m_a.

Here, θ is the inclination angle of the tangent SZ of deflection curve at S to the z axis, and θ_x, θ_y are the projectional angles of θ to planes xz and yz. Now let us define another system $O_a-x_a y_a z$, which is the rectangular coordinate system through O_a paralleling the system O-xyz.

Internal and external damping of the shaft is not taken into consideration. The flexible pedestal K is orthogonally linked to two viscous type dashpots D having equal values of damping c.

The analysis covers the steady-state forced vibration of the system and complex

notation z, θ_z, z_a with vector interpretation is used, with $j=\sqrt{-1}$ as the imaginary unit.

$$\left.\begin{aligned} z&=x+jy \\ \theta_z&=\theta_x+j\theta_y \\ z_a&=x_a+jy_a \end{aligned}\right\} \tag{1}$$

Influence numbers of the shaft system a_{ij} are equal to a_{ji} by Maxwell's theorem of reciprocity. Flexibility matrix $[a_{ij}]$ is introduced as follows,

$$\begin{bmatrix} z \\ \theta_z \\ z_a \end{bmatrix}=[a_{ij}]\begin{bmatrix} P \\ Mt \\ P_a \end{bmatrix} \tag{2}$$

in which P is the inertia force of the rotor acting on the shaft at S, Mt is the inertia couple of the rotor acting around the point S, and P_a is the sum of the inertia force of a concentrated mass m_a and the viscous damping force acting on the lower bearing A. The positive direction for Mt agrees with the direction of increasing θ. Stiffness matrix $[\alpha_{ij}]$ is the inverse matrix $[a_{ij}]^{-1}$, and Eq. (2) is transformed into the following:

$$\begin{bmatrix} P \\ Mt \\ P_a \end{bmatrix}=[\alpha_{ij}]\begin{bmatrix} z \\ \theta_z \\ z_a \end{bmatrix} \tag{3}$$

Element α_{ij} $(=\alpha_{ji})$ is stiffness of the system, and K_{ij} is the cofactor of the determinant $|\alpha_{ij}|$ with respect to stiffness element α_{ij}. For the original shaft, both ends of which are supported by rigid pedestals A, B in Fig. 1, Eq. (3) is expressed as Eq. (3′)

$$\begin{bmatrix} P \\ Mt \end{bmatrix}=\begin{bmatrix} \alpha & \gamma \\ \gamma & \delta \end{bmatrix}\begin{bmatrix} z \\ \theta_z \end{bmatrix} \tag{3'}$$

where α, γ and δ are spring constants of the original shaft itself.

Let $e=\overline{SG}$ be the eccentricity of rotor; $\tau=\angle ZSZ_1$ the small deviational angle between the principal axis SZ_1 of polar moment of inertia and the tangent SZ of the deflection curve of shaft at the point S; β the phase angle between directions e and τ; ω the constant angular speed of shaft; I_p the polar moment of rotor inertia around SZ_1 axis, and I the moment of rotor inertia around its diameter.

The displacement z_g of gravitational center G of rotor, and the inclination angle θ_{z1} of the principal axis SZ_1 perpendicular to the plane of the rotor surface are expressed as follows,

$$\left.\begin{aligned} z_g&=z+e\cdot\exp(j\omega t) \\ \theta_{z1}&=\theta_z+\tau\cdot\exp\{j(\omega t+\beta+\pi)\} \end{aligned}\right\} \tag{4}$$

Using Eq. (4), we have P, Mt and P_a,

$$\left.\begin{aligned} P&=P_x+jP_y=-m\ddot{z}_g=-m\ddot{z}+me\omega^2\exp(j\omega t) \\ Mt&=Mt_y-jMt_x=-I\ddot{\theta}_{z1}+jI_p\omega\dot{\theta}_{z1}=-I\ddot{\theta}_z+jI_p\omega\dot{\theta}_z \\ &\qquad +(I_p-I)\tau\omega^2\exp\{j(\omega t+\beta)\} \\ P_a&=P_{ax}+jP_{ay}=-m_a\ddot{z}_a-c\dot{z}_a \end{aligned}\right\} \tag{5}$$

3. Forced Vibrations

Considering only steady-state forced vibrations, we take a particular solution of Eqs. (3), (5) in the form

$$\left.\begin{aligned} z &= E\exp(j\omega t) \\ \theta_z &= F\exp(j\omega t) \\ z_a &= E_a\exp(j\omega t) \end{aligned}\right\} \tag{6}$$

Substituting these expressions into Eqs. (3) and (5), we obtain three amplitudes E, F and E_a in complex notation.

$$\left.\begin{aligned} E &= E_e + E_\tau = \{\Phi_{11} me\omega^2 + \Phi_{21}(I_p - I)\tau\omega^2 \cdot \exp(j\beta)\}/|\phi_{ij}| \\ F &= F_e + F_\tau = \{\Phi_{12} me\omega^2 + \Phi_{22}(I_p - I)\tau\omega^2 \cdot \exp(j\beta)\}/|\phi_{ij}| \\ E_a &= E_{ae} + E_{a\tau} = \{\Phi_{13} me\omega^2 + \Phi_{23}(I_p - I)\tau\omega^2 \cdot \exp(j\beta)\}/|\phi_{ij}| \end{aligned}\right\} \tag{7}$$

In above equations (7) lower suffix e or τ in amplitudes E, F, E_a means amplitude due to static unbalance e or dynamic unbalance τ respectively.

Notation $|\phi_{ij}|$ is a determinant consisting of elements ϕ_{ij} as follows:

$$|\phi_{ij}| = \begin{vmatrix} \alpha_{11} - m\omega^2 & \alpha_{12} & \alpha_{13} \\ \alpha_{21} & \alpha_{22} + (I_p - I)\omega^2 & \alpha_{23} \\ \alpha_{31} & \alpha_{32} & \alpha_{33} - m_a\omega^2 + jc\omega \end{vmatrix} = M + jcN \tag{8}$$

Let the cofactor of determinant $|\phi_{ij}|$ with regard to element ϕ_{ij} be Φ_{ij} expressed in the following form:

$$\omega^2 \Phi_{ij} = G_{ij} + jcH_{ij} \tag{9}$$

In Eqs. (8) and (9), M, N, G_{ij}, H_{ij} are all real and do not contain j. Synchronous unbalance response can be expressed in bilinear form. Thus:

$$\left.\begin{aligned} \frac{E_e}{me} &= \frac{G_{11} + jcH_{11}}{M + jcN} \\ \frac{F_e}{me} &= \frac{G_{12} + jcH_{12}}{M + jcN} = \frac{E_\tau}{(I_p - I)\tau \cdot \exp(j\beta)} \\ \frac{F_\tau}{(I_p - I)\tau \cdot \exp(j\beta)} &= \frac{G_{22} + jcH_{22}}{M + jcN} \end{aligned}\right\} \tag{10}$$

$$\left.\begin{aligned} \frac{E_{ae}}{me} &= \frac{G_{13}}{M + jcN} \\ \frac{E_{a\tau}}{(I_p - I)\tau \cdot \exp(j\beta)} &= \frac{G_{23}}{M + jcN} \end{aligned}\right\} \tag{10'}$$

4. Fixed Points in Response Curve and Optimum Damping

4. 1. Forced vibrations of rotor E_e, F_e, E_τ, F_τ

The absolute value of Eq. (10) is expressed in the same form as a rectilinear-vibratory system of two degrees of freedom with damping [6],

$$\left|\frac{G_{ij}+jcH_{ij}}{M+jcN}\right|=\sqrt{\frac{G_{ij}^2+c^2H_{ij}^2}{M^2+c^2N^2}} \quad (ij=11,\ 12,\ 22) \tag{11}$$

This amplitude is independent of the damping c if $G^2{}_{ij}\,N^2-H^2{}_{ij}\,M^2=0$, or

$$\left|\frac{G_{ij}}{M}\right|=\left|\frac{H_{ij}}{N}\right| \tag{12}$$

Or again, if Eq. (12) is written out separately:

$$G_{ij}N-H_{ij}M=0 \tag{12. a}$$

$$G_{ij}N+H_{ij}M=0 \tag{12. b}$$

Algebraic equations (12. a), (12. b) in variable ω give the horizontal coordinates of fixed points through which all curves for various values of damping pass in the resonace diagram (see Fig. 2).

By taking $c=0$ we obtain response curve $|G_{ij}/M|$ from Eq. (11). Critical speeds ω_c for this system are obtained by equating the denominator M to zero. Another extreme case $|H_{ij}/N|$ is defined by taking $c=\infty$. If damping is infinitely large, critical speed ω_γ is derived by equating the denominator N to zero. For any other value of damping the response curve falls between the response curves $|G_{ij}/M|$ and $|H_{ij}/N|$.

The most favorable response curve is the one which passes with a horizontal tangent through the highest among the fixed points. Then the best obtainable amplitude becomes the vertical coordinate of the highest. Differentiate the amplitude (11) with respect to ω, thus finding the slope, and then equate said slope to zero for the fixed points:

$$\frac{\partial}{\partial\omega}\sqrt{\frac{G_{ij}^2+c^2H_{ij}^2}{M^2+c^2N^2}}= \frac{(G_{ij}G'_{ij}+c^2H_{ij}H'_{ij})(M^2+c^2N^2)-(MM'+c^2NN')(G_{ij}^2+c^2H_{ij}^2)}{\sqrt{(G_{ij}^2+c^2H_{ij}^2)(M^2+c^2N^2)^3}}=0 \tag{13}$$

Then the equations (14. a), (14. b) for optimum damping c_{opt} can be obtained by using Eqs. (12. a), (12. b) respectively.

$$c_{opt}^2=-\frac{M(G'_{ij}M-G_{ij}M')}{N(H'_{ij}M-G_{ij}N')} \tag{14. a}$$

$$c_{opt}^2=\frac{M(G'_{ij}M-G_{ij}M')}{N(H'_{ij}M+G_{ij}N')} \tag{14. b}$$

Prime over G_{ij}, etc. in Eqs. (13), (14) indicates differentiation with respect to ω.

Dimensionless symbols $\zeta=c/\sqrt{m\alpha}$, $\zeta_{opt}=c_{opt}/\sqrt{m\alpha}$ are introduced in the following.

4. 1. 1. Displacement response of rotor E_e due to static unbalance e

By substituting lower suffix $ij=11$ into Eq. (12. a) and using M, N, G_{11} and H_{11} from Eqs. (8), (9), the abscissas of fixed points are obtained in the more simplified form

$$\omega^2=\frac{K_{13}}{(I_p-I)\alpha_{13}} \tag{15. a}$$

excepting $\omega=0$ at which amplitude E_e is always zero independently of damping.

For a shaft with uniform bending stiffness EI_o and $I_o=\pi d^4/64$ both ends of which are simply supported by self-aligning double-row ball bearings as shown in Fig. 1, $K_{13}/\alpha_{13}=-b\ (\alpha\delta-\gamma^2)/(\alpha b-\gamma)=-3lEI_o/b^2<0$ always holds, and then Eq. (15. a) is negative and has a purely imaginary root, and Eq. (12. a) gives no fixed point since the $I_p>I$ rotor is used in our experiment.

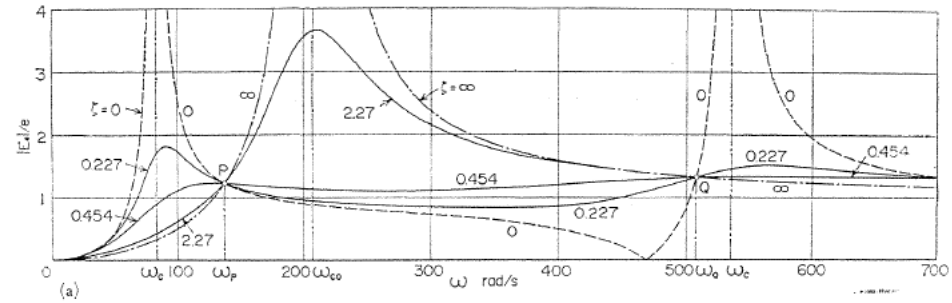

$|E_e|/e$ versus ω

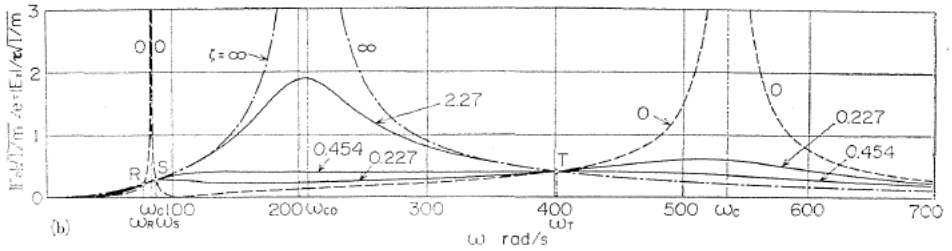

$|F_e|\sqrt{I/m}/e=|E_\tau|/\tau\sqrt{I/m}$ versus ω

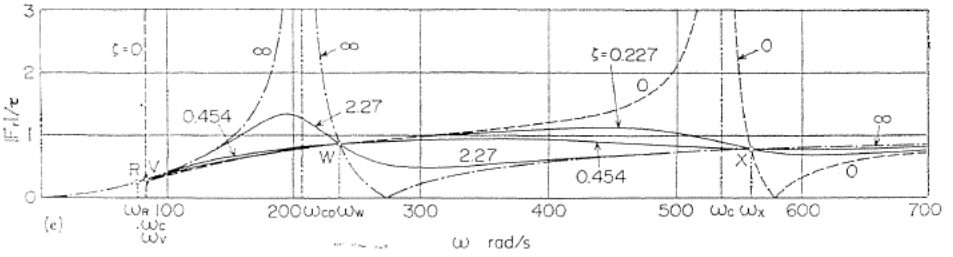

$|F_\tau|/\tau$ versus ω

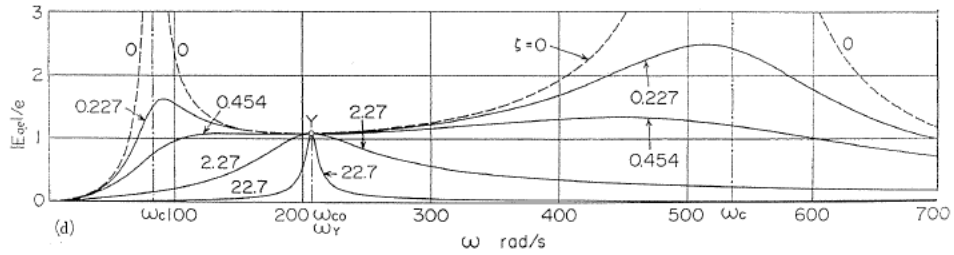

$|E_{ae}|/e$ versus ω

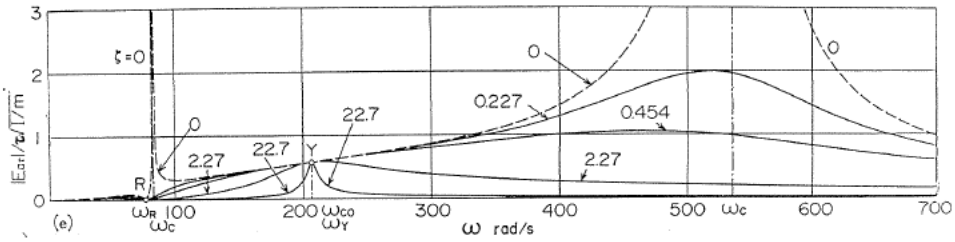

$|E_{a\tau}|/\tau\sqrt{I/m}$ versus ω

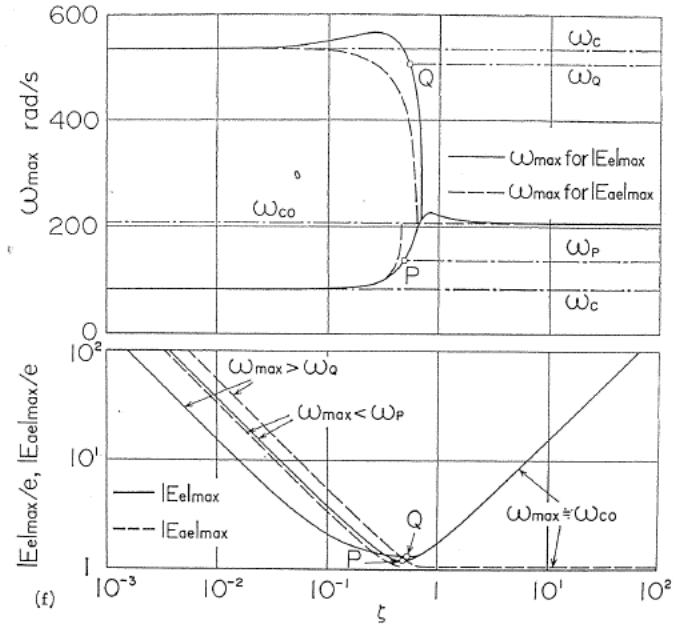

$|E_e|_{max}$, $|E_{ae}|_{max}$, ω_{max} versus dimensionless damping ζ

Fig. 2. Rotor response $|E_e|$, $|F_e|$, $|E_\tau|$, $|F_\tau|$ and pedestal response $|E_{ae}|$, $|E_{a\tau}|$ versus rotating speed ω for various amounts of damping; system shown in Fig. 1, Fig. 7 (a) and Fig. 8.
($m_a/m=0.309$, $k_a/\alpha=0.1115$, $\xi_{PQ}=1.08$, $\zeta_P=0.483$, $\zeta_Q=0.532$, $|E_e|_P/e=1.23$, $|E_e|_Q/e=1.33$, $|E_{ae}|_Y/e=1.09$)

Expansion of Eq. (12. b) by putting lower suffix $ij=11$ in Eqs. (8), (9) yields

a quartic equation (15. b) in the variable ω^2,

$$
\begin{aligned}
&2mm_a(I_p-I)^2\omega^8\\
&+2(I_p-I)\{2mm_a\alpha_{22}-m(I_p-I)\alpha_{33}-m_a(I_p-I)\alpha_{11}\}\omega^6\\
&+\{2mm_a\alpha_{22}^2-2m(I_p-I)(\alpha_{22}\alpha_{33}+K_{11})-2m_a(I_p-I)(\alpha_{11}\alpha_{22}+K_{33})\\
&+(I_p-I)^2(\alpha_{11}\alpha_{33}+K_{22})\}\omega^4\\
&+\{-2m\alpha_{22}K_{11}-2m_a\alpha_{22}K_{33}+(I_p-I)(\alpha_{11}K_{11}+\alpha_{22}K_{22}+\alpha_{33}K_{33}+|\alpha_{ij}|)\}\omega^2\\
&+\alpha_{22}|\alpha_{ij}|+K_{11}K_{33}=0
\end{aligned}
\qquad (15.\ b)
$$

This equation gives the abscissas ω_P, ω_Q of the fixed points P and Q in Fig. 2 (a). Displacement response of rotor E_e against angular speed ω is shown in Fig. 2 (a) for various values of damping: $c=0$, 0.5, 1, 5, 50 or ∞ kg s/cm. Dimensions and spring constants for calculation of Figs. 2 (a)$\sim$(f) are those with the experimental apparatus (Fig. 8), and the abscissas of fixed points P, Q are calculated numerically from Eq. (15. b) as $\omega_P=137.4$ rad/s, $\omega_Q=507.3$ rad/s. The ordinates $|E_e|_P$, $|E_e|_Q$ of fixed points P, Q are given respectively by the first equation of Eq. (10) as

$$
\frac{|E_e|_{P,Q}}{me}=\left|\frac{G_{11}}{M}\right|_{\omega=\omega_P,\,\omega_Q}=\left|\frac{H_{11}}{N}\right|_{\omega=\omega_P,\,\omega_Q} \qquad (10.\ 1)
$$

The optimum damping c_P or c_Q making the tangent to the resonance curve horizontal at P or Q, is separately given by Eq. (14. b) by letting $ij=11$ and $\omega=\omega_P$ or $\omega=\omega_Q$.

Fig. 2 (f) shows the maximum values $|E_e|_{max}$, $|E_{ae}|_{max}$ and rotating speed of peak ω_{max} against the various damping ζ from 10^{-3} to 10^2. The maximum value of amplitude $|E_e|_{max}$ makes a flat bottom near the optimum dampings $\zeta_P=0.483$, $\zeta_Q=0.532$. It makes little difference in $|E_e|_{max}$ and $|E_{ae}|_{max}$, even if the adopted value of damping ζ differs to some extent from Eq. (20).

4. 1. 2. Rotor response F_e due to static unbalance e, or E_τ due to dynamic unbalance τ

When lower suffix $ij=12$ is introduced into Eq. (12. a), the abscissas of fixed points in response F_e, E_τ in relation to ω are given by both Eq. (15. a) and the following equation,

$$
\omega^2=-\frac{K_{23}}{m\alpha_{23}} \qquad (16.\ a)
$$

Since the relation $K_{23}/\alpha_{23}=-(\alpha\delta-\gamma^2)/(\delta-\gamma b)=-3lEI_o/ab^3<0$ always holds for a simply supported shaft with uniform bending stiffness EI_o, as shown in Fig. 1, Eq. (16. a) is positive and has a real root ($\omega_R=76.6$ rad/s). The abscissa ω_R of fixed point R is not only independent of m_a, but also independent of k_a for the shaft system shown in Fig. 1, as Eq. (16. a) does not include m_a and k_a.

Expansion of Eq. (12. b) by putting $ij=12$ in Eqs. (8), (9) yields a cubic equation (16. b) in the variable ω^2

$$
\begin{aligned}
&2mm_a(I_p-I)\alpha_{12}\omega^6\\
&+\{2mm_a\alpha_{12}\alpha_{22}-m(I_p-I)(\alpha_{12}\alpha_{33}-K_{12})-2m_a(I_p-I)\alpha_{11}\alpha_{12}\}\omega^4
\end{aligned}
$$

$$-\{m(\alpha_{12}K_{11}-\alpha_{22}K_{12})+2m_a\alpha_{12}K_{33}+(I_p-I)(\alpha_{11}K_{12}-\alpha_{12}K_{22})\}\omega^2$$
$$+\alpha_{12}|\alpha_{ij}|-K_{12}K_{33}=0 \qquad (16.\ b)$$

Equation (16. b) has two real roots, $\omega_S=86.8$ rad/s and $\omega_T=401.6$ rad/s. The ordinates $|F_e|_{R,\,S,\,T}$ or $|E_\tau|_{R,\,S,\,T}$ at the fixed points R, S, T in Fig. 2 (b) are given by the second equation of Eq. (10) as

$$\frac{|F_e|_{R,\,S,\,T}}{me}=\frac{|E_\tau|_{R,\,S,\,T}}{|I_p-I|\tau}=\left|\frac{G_{12}}{M}\right|_{\omega=\omega_R,\,\omega_S,\,\omega_T}=\left|\frac{H_{12}}{N}\right|_{\omega=\omega_R,\,\omega_S,\,\omega_T} \qquad (10.\ 2)$$

The optimum damping c_R, giving the horizontal tangent to response at R, is given by Eq. (14. a) from letting $ij=12$ and $\omega=\omega_R$, but the optimum dampings c_S, c_T at fixed points S, T are derived from different equation (14. b) letting $ij=12$ and $\omega=\omega_S$, ω_T.

4. 1. 3. Inclination response of rotor $F\tau$ due to dynamic unbalance τ

Substituting lower suffix $ij=22$ into Eq. (12. a) yields the same equation as Eq. (16. a) with the abscissa $\omega_R=76.6$ rad/s.

Equation (12. b) is transformed into a quartic equation (17. b) in the variable ω^2,

$$2m^2m_a(I_p-I)\omega^8$$
$$+2m\{mm_a\alpha_{22}-m(I_p-I)\alpha_{33}-2m_a(I_p-I)\alpha_{11}\}\omega^6-\{m^2(\alpha_{22}\alpha_{33}+K_{11})$$
$$+2mm_a(\alpha_{11}\alpha_{22}+K_{33})-2m(I_p-I)(\alpha_{11}\alpha_{33}+K_{22})-2m_a(I_p-I)\alpha_{11}^2\}\omega^4$$
$$+\{m(\alpha_{11}K_{11}+\alpha_{22}K_{22}+\alpha_{33}K_{33}+|\alpha_{ij}|)+2m_a\alpha_{11}K_{33}-2(I_p-I)\alpha_{11}K_{22}\}\omega^2$$
$$-\alpha_{11}|\alpha_{ij}|-K_{22}K_{33}=0 \qquad (17.\ b)$$

Equation (17. b) has three real roots $\omega_V=83.1$ rad/s, $\omega_W=236.6$ rad/s and $\omega_X=558.9$ rad/s. The ordinates $|F_\tau|_{R,\,V,\,W,\,X}$ at fixed points R, V, W, X in Fig. 2 (c) are given by the third equation of Eq. (10) as

$$\frac{|F_\tau|_{R,\,V,\,W,\,X}}{|I_p-I|\tau}=\left|\frac{G_{22}}{M}\right|_{\omega=\omega_R,\,\omega_V,\,\omega_W,\,\omega_X}=\left|\frac{H_{22}}{N}\right|_{\omega=\omega_R,\,\omega_V,\,\omega_W,\,\omega_X} \qquad (10.\ 3)$$

The optimum damping c_R at R is derived from Eq. (14. a) by letting $ij=22$ and $\omega=\omega_R$; on the contrary, the optimum dampings c_V, c_W, c_X at V, W, X are derived from Eq. (14. b) by putting $ij=22$ and $\omega=\omega_V$, ω_W, ω_X separately.

4. 2. Forced vibrations of flexible pedestal E_{ae}, $E_{a\tau}$

The absolute value of Eq. (10′) is expressed in the same form as Eq. (11), excepting $H_{i3}=0$.

$$\left|\frac{G_{i3}}{M+jcN}\right|=\sqrt{\frac{G_{i3}^2}{M^2+c^2N^2}} \quad (i=1,\ 2) \qquad (11')$$

This is independent of the damping c if G_{i3} $N=0$, or written out separately if

$$G_{i3}=0 \qquad (12.\ c)$$
$$N=\omega\Phi_{33}=\omega[m(I_p-I)\omega^4+\{m\alpha_{22}-(I_p-I)\alpha_{11}\}\omega^2-\alpha_{11}\alpha_{22}+\alpha_{12}^2]=0 \qquad (12.\ d)$$

At the abscissa of the fixed point R satisfying Eq. (12. c), the ordinate $|E_a|_R$ is always zero by Eq. (11′), and it counts for nothing.

As the abscissa ω_Y of fixed point Y is obtained by equating Eq. (12. d), that is, the denominator of response $|H_{ij}/N|$ to zero, ω_Y is naturally nothing but the critical speed for infinitely large damping. Unless the dashpots D are connected to the original shaft St through a ball bearing C other than A as in Figs. 7 (c), (d), ω_Y coincides with the former critical speed ω_{co} of the original shaft, satisfying $\alpha_{11}=\alpha$, $\alpha_{12}=\gamma$, $\alpha_{22}=\delta$ in Eq. (12. d).

The tangent through the fixed point Y is derived by introducing $H_{ij}=0$ and $N=0$ into Eq. (13) as follows,

$$\left(\frac{\partial}{\partial\omega}\sqrt{\frac{G_{i3}^2}{M^2+c^2N^2}}\right)_{\omega=\omega_Y}=\pm\frac{(G'_{i3}M-G_{i3}M')}{M^2}$$

according to $G_{i3}M\gtrless O$. The tangent at Y is found to have no connection with damping c. Equating the tangent at Y to zero gives the following relation:

$$G'_{i3}M-G_{i3}M'=0 \qquad (13.\ d)$$

Even if a horizontal tangent is given to the response curve through Y, there may be two peaks ($\omega\fallingdotseq\omega_c=83.0$, 535.4 rad/s) on either side of Y in the case of small damping as shown in Fig. 2 (d), (e). Then the damping c is desirable to be larger than critical damping c_{cr}, and c_{cr} is derived by equating the second differential coefficient of Eq. (11′) to zero and by using Eqs. (12. d), (13. d) as follows,

$$c_{cr}^2=\frac{G''_{i3}M^2+G'_{i3}MM'-G_{i3}(M'^2+MM'')}{G_{i3}N'^2} \qquad (14.\ d)$$

4. 2. 1. Displacement response of flexible pedestal E_{ae} due to static unbalance e

Substituting $i=1$ into Eq. (12. c) gives the same equation as Eq. (15. a), which yields no fixed point in Fig. 2 (d) regarding the $I_p>I$ rotor used.

The abscissa ω_Y is given by Eq. (12. d), and the ordinate $|E_{ae}|_Y$ is obtained from the first equation of Eq. (10′). For the apparatus shown in Fig. 8, $\omega_Y=207.1$ rad/s and $|E_{ae}|_Y/e=1.09$ are found to be definitely independent of m_a and k_a because $\omega_Y=\omega_{co}$.

Inserting $k_a/\alpha=0.1115$ into Eq. (13. d) determines a mass ratio $m_a/m=0.269$, which makes a horizontal tangent through the fixed point Y. Moreover, inserting the combination of $k_a/\alpha=0.1115$ and $m_a/m=0.269$ into Eq. (14. d) defines a critical damping $\zeta_{cr}=0.550$.

4. 2. 2. Displacement response of flexible pedestal $E_{a\tau}$ due to dynamic unbalance τ

Introducing $i=2$ into Eq. (12. c) yields Eq. (16. a), which has a real root, $\omega_R=76.6$ rad/s. Fixed point R lies on the horizontal coordinate as shown in Fig. 2 (e).

There exists another fixed point Y, the ordinate of which $|E_{a\tau}|_Y/\tau\sqrt{I/m}=0.57$ is also found to be independent of m_a and k_a for the shaft system in Fig. 1 where the relation $\omega_Y=\omega_{co}$ always holds.

5. Favorable Choice of Added Mass m_a and Pedestal Stiffness k_a

5. 1. Tuning condition adjusting rotor response to zero at critical speed ω_{co} of original shaft

Even if the flexible pedestal has no damping, an appropriately chosen combination of m_a and k_a can bring rotor response E or F to zero at the angular speed $\omega=\omega_{co}$, which is nothing but the resonant speed of the original shaft rigidly supported by lower and upper pedestals A and B.

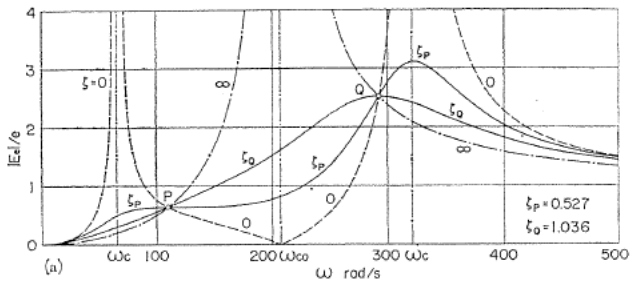

$|E_e|/e$ versus ω

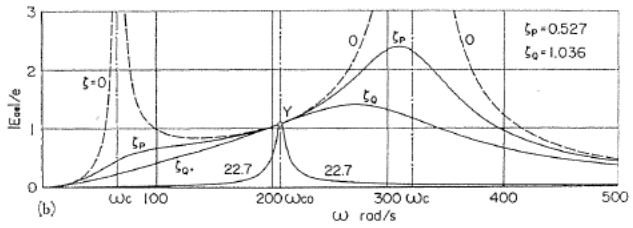

$|E_{ae}|/e$ versus ω

Fig. 3. Response curves $|E_e|-\omega$, and $|E_{ae}|-\omega$ for a favorable case derived by letting amplitude $E_e=0$ at $\omega=\omega_{co}=207.1$ rad/s.
($m_a/m=1.062$, $k_a/\alpha=0.1115$, $\xi_{PQ}=3.94$, $\zeta_P=0.527$, $\zeta_Q=1.036$)

Inserting the critical speed $\omega=\omega_{co}$ into Eq. (8) and assuming G_{11} is zero gives the following relation between m_a and k_a,

$$m_a=\frac{(I_p-I)\alpha_{33}\omega_{co}^2+K_{11}}{\omega_{co}^2\{(I_p-I)\omega_{co}^2+\alpha_{22}\}} \tag{18}$$

A chain-line curve in Fig. 4 (a) represents the mass ratio m_a/m as the function of k_a/α for the shaft (Fig. 8). Mass ratio $m_a/m=1.062$ is defined by Eq. (18) for a given stiffness ratio $k_a/\alpha=0.1115$.

Figs. 3 (a), (b) show response curves $E_e-\omega$ and $E_{ae}-\omega$ for a flexible pedestal K with parameters of $m_a/m=1.062$ and $k_a/\alpha=0.1115$. The amplitude E_e is made zero at the former critical speed $\omega_{co}=207.1$ rad/s. A response curve ($E_e-\omega$) of infinitely large damping coincides with that of the original shaft.

We can obtain tuning conditions similar to Eq. (18) with respespect to F_e, E_τ, and F_τ. These conditions are effectively applied to the vibration-proof problem of

rotor response only if the running speed of the shaft is limited to a rather narrow speed range near $\omega=\omega_{co}$. Moreover, it is dangerous for the no damping shaft to be increased or decreased repeatedly passing through the first critical speed ω_c lower than ω_{co}.

When the viscous type dashpots of optimum damping ζ_{opt} are equipped with the flexible pedestal K, the value ζ_Q in Fig. 3 is seen to be twice as much as ζ_P, and the ordinate $|E_e|_Q$ of the fixed point Q is four times larger than $|E_e|_P$ of fixed point P as shown by chain lines in Fig. 4 (c). Even if we choose the larger value $\zeta_Q=1.036$ between ζ_P and ζ_Q for the response curve $E_e-\omega$ of Fig.3 (a), we cannot get one as flat as in Fig. 2 (a).

5. 2. Most favorable condition for equality of ordinates of fixed points

By changing a combination of m_a and k_a one point between fixed points P and Q goes up, and the other down. The most favorable case is clearly one in which, by a proper choice of m_a and k_a, the two fixed points P and Q are adjusted to equal heights $|E_e|_P=|E_e|_Q$, and by a proper choice of damping ratio (ζ_{opt}) the response curve is adjusted to pass through one of them with a horizontal tangent. It will be shown later in Fig. 4 (d) that it makes practically no difference which one of the

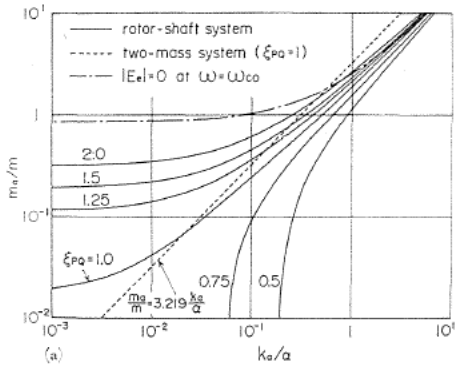

m_a/m versus k_a/α

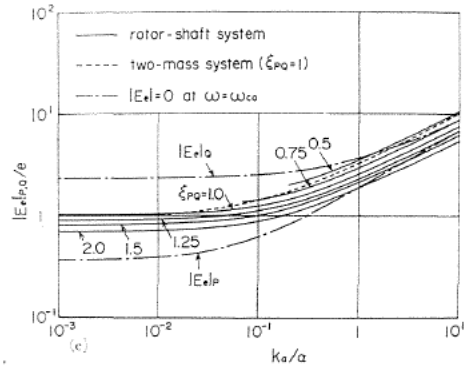

$|E_e|_{P,Q}/e$ versus k_a/α

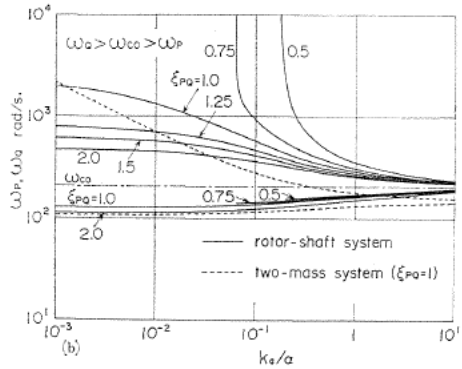

ω_P, ω_Q versus k_a/α

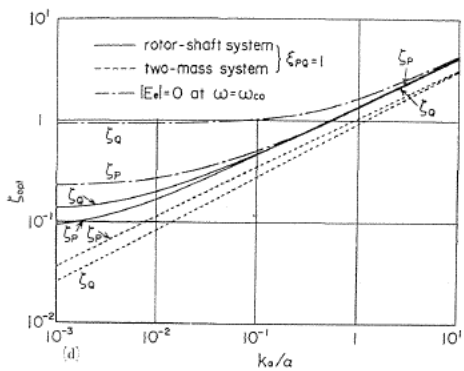

ζ_{opt} versus k_a/α

Fig. 4. The most favorable choice of m_a/m, k_a/α, and optimum damping ζ_{opt} as regards rotor response $|E_e|$ due to static unbalance e.

two we choose, ζ_P or ζ_Q.

Any choice of m_a and k_a in Fig. 4 (a) gives the two fixed points P and Q, the ordinates of which are not always equal. A parameter ξ_{PQ} is introduced as the ratio of the two ordinates,

$$|E_e|_Q=\xi_{PQ}|E_e|_P \tag{19}$$

The abscissas ω_P, ω_Q of fixed points P, Q can be given numerically by Eq. (15. b). The ordinate $|E_e|_P$ of fixed point P and the ratio ξ_{PQ} are derived from Eq (10. 1). They are plotted for various ratios $\xi_{PQ}=0.5\sim2.0$ by full-line curves in Figs. 4 (b), (c).

The most favorable case is denoted by full-line curves ($\xi_{PQ}=1$) in Figs. 4 (a), (b), (c) and (d). It is clearly seen from Fig. 4 (a) that some deviation (m_a or k_a) from the most favorable case $\xi_{PQ}=1$ curve) makes practically no large difference between $|E_e|_P$ and $|E_e|_Q$, especially when the pedestal stiffness ratio k_a/α is smaller than 0.1. Fig. 4 (c) shows that the ordinate $|E_e|_P/e$ remains nearly at unity in relation to the values k_a/α from 10^{-3} to 10^{-1}. On the contrary, the decrease of the ratio k_a/α smaller than 0.1 makes a difference between optimum dampings ζ_P and ζ_Q in Fig. 4 (d). By taking Figs. 4 (a), (c) and (d) into consideration, we may determine the most proper stiffness of the flexible pedestal to be approximately $k_a/\alpha=0.1$.

Either choice of $m_a/m=0.266$ and $k_a/\alpha=0.1115$, or $m_a/m=0.309$ and $k_a/\alpha=0.133$ can make the ordinate ratio of fixed points P, Q equal to unity, that is, $\xi_{PQ}=1$ for the shaft (Fig. 8). Although a flexible pedestal K with $m_a/m=0.309$ and $k_a/\alpha=0.1115$ is used in our experiment and shows a slight deviation from the most favorable case ($m_a/m=0.266$ and $k_a/\alpha=0.1115$), it makes little difference in heights ($\xi_{PQ}=1.08$), and also the optimum dampings ($\zeta_P=0.483$, $\zeta_Q=0.532$) deviate little from the most favorable case ($\zeta_P=0.486$, $\zeta_Q=0.495$).

5. 2. 2. F_e or E_τ

When the most favorable case for E_e shown by a full-line curve $\xi_{PQ}=1$ in Fig. 5 (a) is applied to rotor response F_e or E_τ, the ordinates $|F_e|_{R,S,T}$ of three fixed points R, S, T are represented by full-line curves against k_a/α in Fig. 5 (b), and the optimum damping ζ_{opt} for the highest fixed point among R, S, T in Fig. 5 (b)

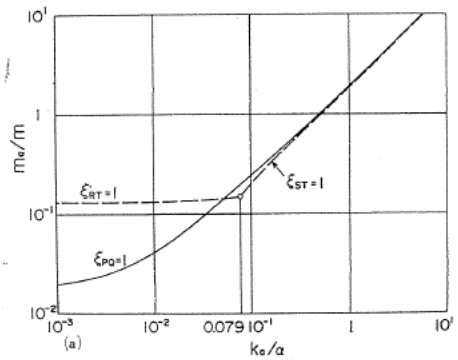

m_a/m versus k_a/α

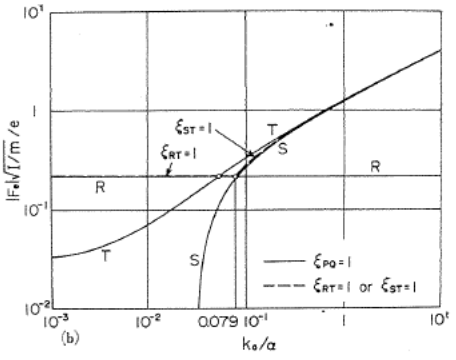

$|F_e|\sqrt{I/m}/e=|E_\tau|/\tau\sqrt{I/m}$ versus k_a/α

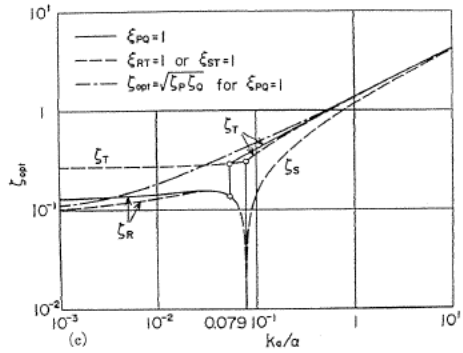

ζ_{opt} versus k_a/α

Fig. 5. Comparison of the most favorable case for E_e with that for F_e.

is also indicated by a full-line discontinuous curve in Fig. 5 (c). Moreover, a chain-line curve in Fig. 5 (c) represents the geometric mean (20) of optimum dampings ζ_P and ζ_Q for $\xi_{PQ}=1$,

$$\zeta_{opt}=\sqrt{\zeta_P\cdot\zeta_Q} \tag{20}$$

Broken-line curves in Figs. 5 (a), (b), (c) are independently derived by the most favorable case so that $\xi_{RT}=|F_e|_T/|F_e|_R=1$ holds for $k_a/\alpha<0.079$, or $\xi_{ST}=|F_e|_T/|F_e|_S=1$ holds for $k_a/\alpha>0.079$ respectively. As the abscissa ω_R agrees with ω_S in the neighborhood of $k_a/\alpha=0.079$, both optimum dampings ζ_R and ζ_S drop sharply in Fig. 5 (c).

There is little difference in Fig. 5 (b) between the largest height R or T among full-line curves (for $\xi_{PQ}=1$) and a broken-line curve (for $\xi_{RT}=1$ or $\xi_{ST}=1$). The optimum damping ζ_{opt} shown by broken-line or full-line curves in Fig. 5 (c) differs little from a chain-line curve of Eq. (20), so the latter may be used in place of the former, taking Fig. 2 (f) into consideration.

5. 2. 3. F_τ

The most favorable case for rotor response F_τ is discussed in the same way as rotor response F_e. When a proper choice of m_a and k_a ($\xi_{PQ}=1$ in Fig. 6 (a))

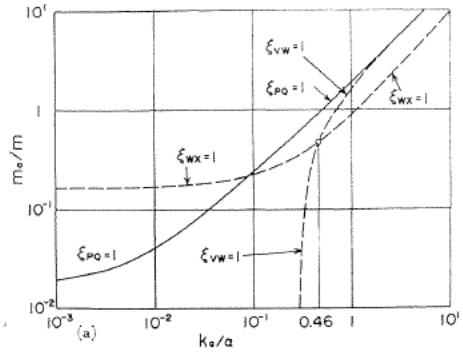

m_a/m versus k_a/α

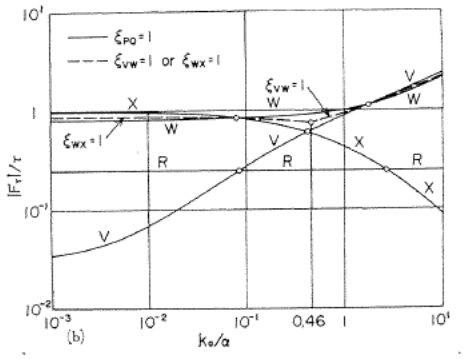

$|F_\tau|/\tau$ versus k_a/α

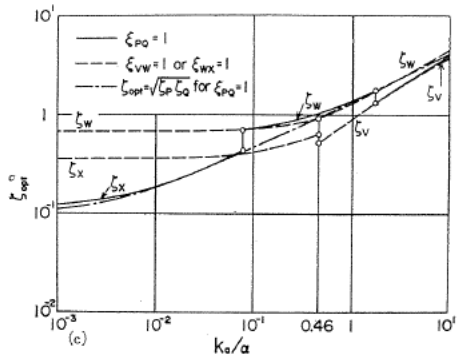

ζ_{opt} versus k_a/α

Fig. 6. Comparison of the most favorable case for E_e with that for F_τ.

is applied to F_τ, the ordinates $|F_\tau|_{R,V,W,X}$ of the four fixed points R, V, W, X are represented by full-line curves in Fig. 6 (b); and also the optimum damping ζ_{opt} for the highest fixed point among R, V, W, X are shown in Fig. 6 (c) by full-line curves. A chain-line curve of Fig. 6 (c) represents the mean of ζ_P and ζ_Q according to Eq. (20), which differs slightly from broken- or full-line curves.

Broken-line curves in Figs. 6 (a), (b), (c) are derived separately by the most favorable case so that $\xi_{WX}=|F_\tau|_X/|F_\tau|_W=1$ holds for $k_a/\alpha<0.46$, or $\xi_{VW}=|F_\tau|_W/|F_\tau|_V=1$ holds for $k_a/\alpha>0.46$. The relation $|F_\tau|_V=|F_\tau|_W=|F_\tau|_X$ exists only if $k_a/\alpha=0.46$ holds.

6. Two-mass System with Damping

By neglecting the inertia couple of rotor Mt and omitting inclination angle θ_z, the rotor-shaft system (Fig. 1 and Fig. 7 (a)) can be simplified to a rectilinear two-mass system with damping (Fig. 7 (e)) which has two degrees of freedom,

$$\begin{bmatrix} z \\ z_a \end{bmatrix}=\begin{bmatrix} a_{11} & a_{13} \\ a_{31} & a_{33} \end{bmatrix}\begin{bmatrix} P \\ P_a \end{bmatrix} \tag{2'}$$

This is rewritten by stiffness matrix,

$$\begin{bmatrix} P \\ P_a \end{bmatrix}=\begin{bmatrix} k_{11} & k_{13} \\ k_{31} & k_{33} \end{bmatrix}\begin{bmatrix} z \\ z_a \end{bmatrix} \tag{3''}$$

In the same analytical way as [6], we can directly obtain abscissas and ordinates of fixed points P, Q as follows,

$$\left.\begin{aligned} \frac{\omega_P^2}{\omega_Q^2} &= \frac{m_a k_{11}+mk_{33}\mp\sqrt{(m_a k_{11}-mk_{33})^2+2mm_a k_{13}^2}}{2mm_a} \\ \frac{|E_e|_{P,Q}}{me} &= \left|\frac{\omega^2}{k_{11}-m\omega^2}\right|_{\omega=\omega_P,\,\omega_Q} \end{aligned}\right\} \tag{21}$$

Substituting $\omega_Y=\sqrt{k_{11}/m}$ into E_{ae} determines the ordinate of fixed point Y,

$$\frac{|E_{ae}|_r}{e}=\left|\frac{k_{11}}{k_{13}}\right| \tag{22}$$

The most favorable case ($\xi_{PQ}=1$) is found to be expressed in the simple form,

$$\frac{m_a}{m}=\frac{k_{11}k_{33}-k_{13}^2}{k_{11}^2} \tag{23}$$

Substituting Eq. (23) into Eq. (21) yields

$$\left.\begin{aligned}\frac{\omega_P^2}{\omega_Q^2}&=\frac{k_{11}\{2k_{11}k_{33}-k_{13}^2\mp\sqrt{k_{13}^2(2k_{11}k_{33}-k_{13}^2)}\}}{2m(k_{11}k_{33}-k_{13}^2)}\\ \frac{|E_e|_P}{e}&=\frac{|E_e|_Q}{e}=\frac{2k_{11}k_{33}-k_{13}^2-\sqrt{k_{13}^2(2k_{11}k_{33}-k_{13}^2)}}{\sqrt{k_{13}^2(2k_{11}k_{33}-k_{13}^2)}-k_{13}^2}\end{aligned}\right\} \tag{24}$$

Using elasticity elements $a_{11}=1/k+(b/l)^2/k_a$, $a_{13}=(b/l)/k_a$ and $a_{33}=1/k_a$ for a simply supported shaft (Fig. 7 (e)) makes

$$k_{11}=k,\quad k_{13}=-(b/l)k,\quad k_{33}=k_a+(b/l)^2k \tag{3'''}$$

where $k=(\alpha\delta-\gamma^2)/\delta=(1/a_{11})_{k_a=\infty}$ is spring constant of the original shaft. Introducing Eq. (3''') into Eq. (22) gives $|E_{ae}|_r/e=l/b=1.25$, which differs little from $|E_{ae}|_r/e=1.09$ for rotor-shaft system (Fig. 2 (d)). By using Eq. (3'''), Eq. (23) is simplified to the formula $m_a/m=k_a/k=(\alpha/k)(k_a/\alpha)=3.219(k_a/\alpha)$, which is denoted by a dotted straight line in Fig. 4 (a). Dotted-line curves in Figs. 4 (b), (c) also represent the values ω_P, ω_Q and $|E_e|_P$ of Eq. (24) for the most favorable case of a two-mass system.

Optimum dampings ζ_P, ζ_Q can be derived from Eq. (14. b) by latting $ij=11$ and introducing $M=(k_{11}-m\omega^2)(k_{33}-m_a\omega^2)-k_{13}^2$, $N=\omega(k_{11}-m\omega^2)$, $G_{11}=\omega^2(k_{33}-m_a\omega^2)$, $H_{11}=\omega^3$. Eqs. (14. b), (24) define the optimum dampings ζ_P, ζ_Q for the most favorable case ($\xi_{PQ}=1$) shown by dotted lines in Fig. 4 (d).

By neglecting the inertia couple of rotor Mt, or putting $I_p=I=0$ in Eq. (5) a rotor-shaft system (Fig. 8) with critical speeds $\omega_c=83.01$, 535.4 and $\omega_{co}=207.1$ rad/s can be simplified to a two-mass system (Fig. 7(e)) with critical speeds $\omega_c=82.98$, 302.7 and $\omega_{co}=152.6$ rad/s. Even if there is some difference in regard to higher critical speeds, dotted-line curves ($\xi_{PQ}=1$ for two-mass system) in Figs. 4 (a), (c), (d) agree approximately with full-line curves ($\xi_{PQ}=1$ for rotor-shaft system), and the former may be adopted as a first step numerically to determine the most favorable case of the latter.

7. Stiffness Elements α_{ij}

Stiffness elements α_{ij} used in Chapters 2~5 may be obtained for usual rotor-shaft systems (see Fig. 7) by using the strength of materials.

7. 1. Simply supported shaft (Fig. 7 (a))

$$\left.\begin{aligned}&\alpha_{11}=\alpha,\quad \alpha_{12}=\gamma,\quad \alpha_{13}=(\gamma-\alpha b)/l,\quad \alpha_{22}=\delta\\ &\alpha_{23}=(\delta-\gamma b)/l,\quad \alpha_{33}=k_a+(\alpha b^2-2\gamma b+\delta)/l^2\end{aligned}\right\} \tag{25. a}$$

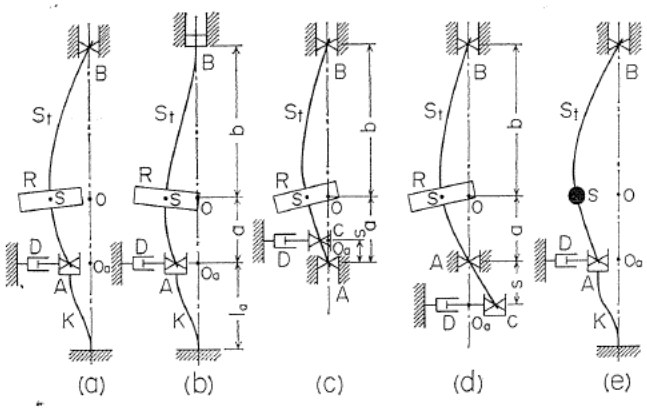

Fig. 7. Various rotor-shaft systems.

7. 2. Clamped-hinged shaft (Fig. 7 (b))

$$\left.\begin{aligned}
&\alpha_{11}=\alpha,\quad \alpha_{12}=\gamma,\quad \alpha_{13}=b\{3\gamma(2l-b)-\alpha b(3l-b)\}/2l^3\\
&\alpha_{22}=\delta,\quad \alpha_{23}=b\{3\delta(2l-b)-\gamma b(3l-b)\}/2l^3\\
&\alpha_{33}=k_a+k_b+[\alpha b^3\{4l^3-a^2(4a+3b)\}-6\gamma b^2\{2l^3-a(2a^2-b^2)\}\\
&\qquad+3\delta b\{4l^3-(4a^3+b^3)\}]/4l^6
\end{aligned}\right\}\qquad (25.\text{b})$$

where k_b is spring constant of cantilever at the location A, letting the upper end B be clamped and the lower end A be free.

7. 3. Dampers connected through ball bearing C to simply supported shaft with uniform bending stiffness (Fig. 7(c))

For $a>s>0$

$$\left.\begin{aligned}
&\alpha_{11}=3EI_0\left\{\frac{1}{b^3}+\frac{4(3a-2s)}{H}\right\},\quad \alpha_{12}=3EI_0\left\{\frac{1}{b^2}-\frac{2(3a-s)(a-s)}{H}\right\}\\
&\alpha_{13}=-6EI_0\frac{(3a^2-s^2)}{sH},\quad \alpha_{22}=3EI_0\left\{\frac{1}{b}+\frac{4a(a-s)^2}{H}\right\}\\
&\alpha_{23}=6EI_0\frac{a(a^2-s^2)}{sH},\quad \alpha_{33}=12EI_0\frac{a^3}{s^2H}
\end{aligned}\right\}\qquad (25.\text{c})$$

where $H=3a^4-8a^3s+6a^2s^2-s^4$

7. 4. Dampers connected through C to overhung uniform shaft on simple supports (Fig. 7 (d))

$$\left.\begin{aligned}
&\alpha_{11}=3EI_0\left\{\frac{1}{b^3}+\frac{4(3a+s)}{a^3(3a+4s)}\right\},\quad \alpha_{12}=3EI_0\left\{\frac{1}{b^2}-\frac{2(3a+2s)}{a^2(3a+4s)}\right\}\\
&\alpha_{13}=\frac{18EI_0}{as(3a+4s)},\quad \alpha_{22}=3EI_0\left\{\frac{1}{b}+\frac{4(a+s)}{a(3a+4s)}\right\}\\
&\alpha_{23}=-\frac{6EI_0}{s(3a+4s)},\quad \alpha_{33}=\frac{12EI_0}{s^2(3a+4s)}
\end{aligned}\right\}\qquad (25.\text{d})$$

8. Experimental Apparatus and Experimental Results

Experimental apparatus is shown in Fig. 8. The rotor R with a diameter of 480 mm and a thickness of 5 mm is driven by a DC motor with speed variations

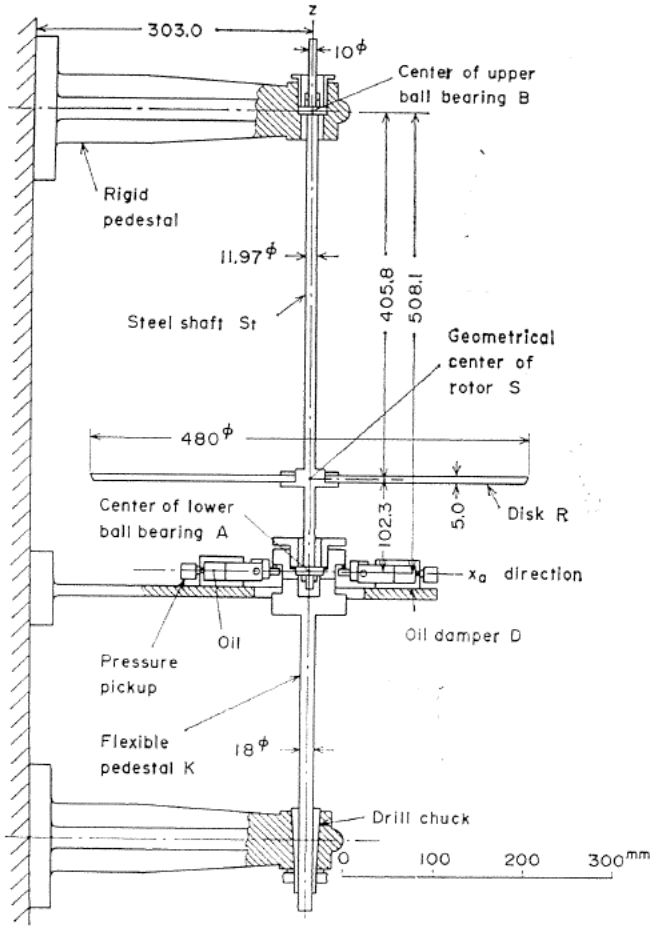

Fig. 8. Experimental apparatus.
(I_p=2.212 kg cm s², I=1.106 kg cm s², mg=7.876 kg, a=10.23 cm, b=40.58 cm, $l=a+b$=50.81 cm, d=1.197 cm, α=602.51 kg/cm, γ=−5680.9 kg/rad, δ=77705 kg cm/rad, ω_{c0}=207.1 rad/s, $\sqrt{\alpha/m}$=273.8 rad/s, $\sqrt{m\alpha}$=2.201 kg s/cm, $\sqrt{I/ml^2}$=0.2309, k/α=1/3.219)

of from 150 rpm to 6000 rpm. In order to eliminate disturbance from the motor a helical spring is inserted between the motor and upper end of a vertical shaft St with a diameter of 11.97 mm. Both ends of shaft are supported freely to incline by self-aligning double-row ball bearings with a bore of 10 mm (#1200). The mass m and moments of inertia I_p, I of rotor, and spring constants α, γ, δ of shaft

itself used in the experiments are indicated in Fig. 8. The shaft is made of mild steel, and α, γ, δ can be obtained from the strength of materials.

The upper surface of the rotor is made of disc, then the whirling of the shaft is measured optically by recording simultaneously lateral motions of the disc edge in both directions x and y. The upper end of shaft B is rigidly supported, while the lower end A is flexibly supported by an isotropically elastic pedestal K with a diameter of 18 mm, the lower end of which is clamped on the rigid base. By changing the length l_a of K, pedestal stiffness k_a can be varied. The value of k_a is directly defined by measurement of deflection at the location A. An equivalently concentrated mass m_a is determined experimentally from the measured natural frequency of the pedestal K only. Two viscous type dampers D are linked orthogonally to the housing of the lower bearing A (see Eig. 9).

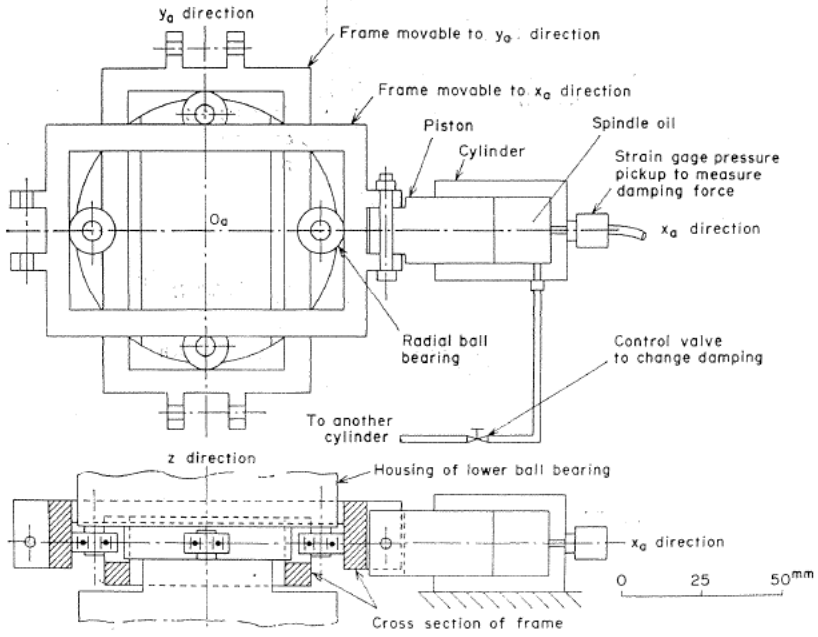

Fig. 9. Pressure-pickup type dashpot.

8. 1. Dampers having nearly equal damping in two directions x_a, y_a

Response curves $E_e-\omega$ and $E_{ae}-\omega$ for a proper choice of $m_a/m=0.309$ and $k_a/\alpha=0.1115$ are obtained experimentally as shown in Figs. 10 (a), (b). Experimental results are indicated by circle marks for various values of damping. Full-line curves ($\zeta=0.0204$ and 0.655) and a chain-line curve ($\zeta=\infty$) are the calculated response curves derived from Eqs. (10) and (10′). Each damper D consists of a cylinder fixed to the ground and a movable piston linked to the bearing housing A. The sliding piston has several holes. Damping force, i. e., pressure difference through piston holes, is measured by a load cell inserted between the cylinder and the ground.

Though there exists little difference in respect to critical speed ω_c between

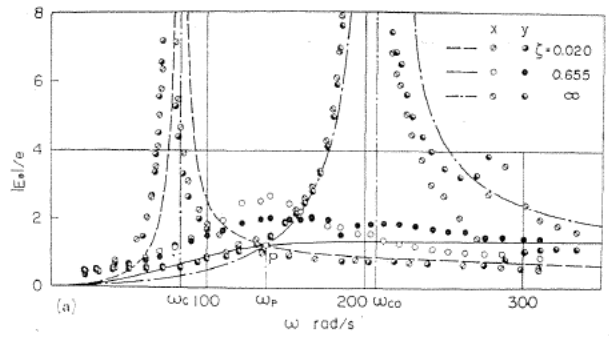

$|E_e|/e$ versus ω

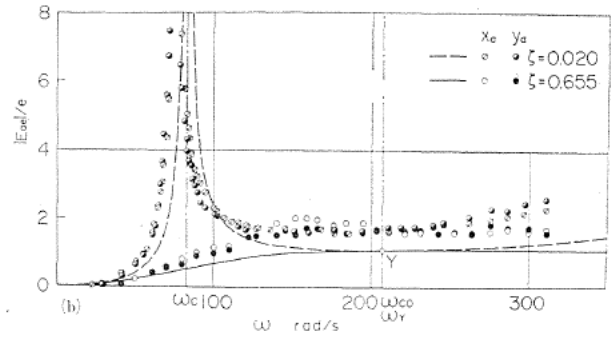

$|E_{ae}|/e$ versus ω

Fig. 10. Response curves with nearly equal damping in two directions x_a, y_a. ($m_a/m=0.309$, $k_a/\alpha=0.1115$)

experimental results and the analytical results because of the accuracy of spring constants, neglect of distributed shaft mass, Coulomb friction in dampers, and some elastic deformation of the load cell, the theoretical results are verified through experiments.

When another choice of $m_a/m=0.340$ and $k_a/\alpha=0.1265$ is adopted, and a pressure pickup of Fig. 9 is inserted into the damper to record the damping forces on behalf of an unavoidably elastic load cell, the experimental response curves

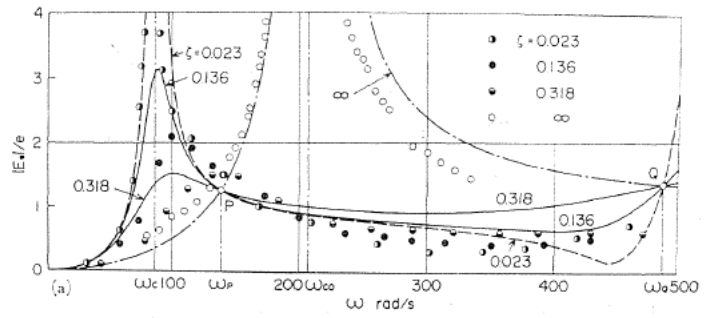

$|E_e|/e$ versus ω

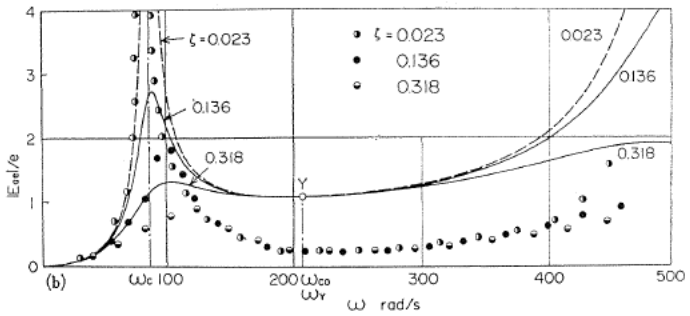

$|E_{ae}|/e$ versus ω

Fig. 11. Response curves with nearly equal damping in two directions x_a, y_a. ($m_a/m=0.340$, $k_a/\alpha=0.1265$)

$E_e-\omega$, $E_{ae}-\omega$ are shown in Eigs. 11 (a), (b). As the damping ζ increases, peak amplitude near $\omega=85$ rad/s decreases, and there clearly appear fixed points P, Q in Fig. 11 (a) and fixed point Y in Fig. 11 (b).

8. 2. Dampers having unequal damping ($\zeta_x<\zeta_y$) in directions x_a, y_a

If the dampers happen to have unequal damping ($\zeta_x<\zeta_y$) in contrary to our expectation, the whirling motions of rotor and flexible pedestal take elliptical paths

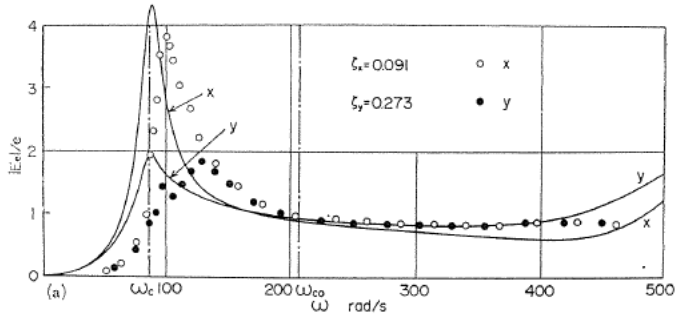

$|E_e|/e$ versus ω

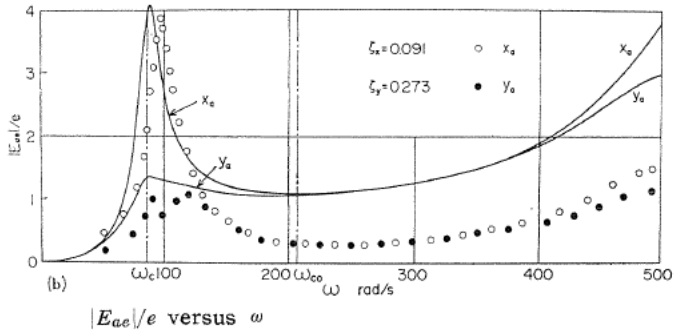

$|E_{ae}|/e$ versus ω

Fig. 12. Response curves with unequal damping in two directions x_a, y_a. ($m_a/m=0.340$, $k_a/\alpha=0.1265$, $\zeta_y/\zeta_x=3$)

near critical speed ω_c, and the major axis of the ellipse motion coincides nearly with x axis. Experimental response curves for a combination of $m_a/m=0.340$ and $k_a/\alpha=0.1265$ are displayed in Figs. 12 (a), (b) where the damping ratio $\zeta_y/\zeta_x=3$. Maximum amplitudes in x direction become two or four times larger than maximum amplitudes in y direction.

9. Conclusions

(1) A flexibly mounted bearing applied to a rotor-shaft system can be very effective to suppress the rotor resonance near the major critical speed.

(1-1) A favorable choice of added mass m_a and pedestal stiffness k_a can make the rotor response to zero at the critical speed ω_{co} of the original shaft only if the running speed of rotor is limited to a narrow range.

(1-2) If a favorable choice of m_a and k_a is adopted so that the fixed points adjusted to equal heights, and if there is a proper choice of damping ζ_{opt} so that the response curve is adjusted to pass through one of the fixed points with a horizontal tangent, the rotor response curve $E_e-\omega$ nearly flattens ous over a wide range of rotating speed.

(1-3) The most favorable choice of m_a, k_a and ζ_{opt} with regard to the displacement response of rotor E_e due to static unbalance e, can be precisely applied to the displacement response of rotor E_τ due to dynamic unbalace τ, and also to the inclination response of rotor $F_\tau$due to τ. Thus, other response curves $E_\tau-\omega$, $F_\tau-\omega$ can also flatten out like $E_e-\omega$ curve.

(2) Fixed point Y in response curve of flexible pedestal generally coincides with the critical speed for infinitely large damping, and the ordinates of the fixed point are constant independently of added mass m_a.

Especially for a rotor-shaft system such as seen in Figs. 7 (a), (b), the abscissa ω_Y coincides with the critical speed ω_{co} of the original shaft, and the ordinate of fixed point Y has no connection with m_a and k_a.

(3) By neglecting the inertia couple of the rotor, a rotor-shaft system is reduced to a two-mass system. Rather simple formulas (23), (24) by the two-mass system can be adopted as a first step numerically to obtain the most favorable case of the rotor-shaft system.

(4) It is most desirable for the flexible pedestal not to have the directional inequality in pedestal stiffness and viscous damping.

The authors wish to express their sincere thanks to Professor Toshio Yamamoto for his guidance and to Mr. Masayoshi Kato for his drawing the figures.

References

1) Tallian, T. E. and Gustafsson, O, G., Progress in Rolling Bearing Vibration Research and Control, Trans. ASLE, Vol. 8, No. 3 (1965), pp. 195—207.

2) Tatara, A., Vibrations and Their Dampers of the Shaft Systems Supported by Ball Bearings, J. Japan Soc. Lubrication Engrs. (in Japanese), Vol. 16, No. 3 (1971),pp. 159—166.

3) Ōta, H., Kōno. K. and Mitsuya, Y., On Elimination of the Unstable Region of the Major Critical Speed in a Rotating Shaft System Carrying an Unsymmetrical Rotor (Dynamical

Effect of a Flexible Pedestal or Added Mass on the Shaft), Bulletin of Japan Soc. Mech. Engrs., Vol. **12**, No. 51 (June 1969), pp. 470—481.

4) Gunter, E. J., Influence of Flexibly Mounted Rolling Element Bearing on Rotor Response (Part 1. Linear Analysis), Trans. ASME, Ser. F, Vol. **92**, No. 1 (Jan. 1970), pp. 59—69.
5) Kirk, R. G. and Gunter, E. J., The Effect of Support Flexibility and Damping on the Synchronous Response of a Single-Mass Flexible Rotor, Trans. ASME, Ser. B, Vol. **94**, No. 1 (Feb. 1972), pp. 221—232.
6) Den Hartog, J. P., Mechanical Vibrations, 4th edition (1956), pp. 93—104, McGraw-Hill Book Company, New York.